

Supplementary Materials for

Room temperature detection of individual molecular physisorption using suspended bilayer graphene

Jian Sun, Manoharan Muruganathan, Hiroshi Mizuta

Published 15 April 2016, *Sci. Adv.* **2**, e1501518 (2016)

DOI: 10.1126/sciadv.1501518

The PDF file includes:

- fig. S1. Optical microscopic image of the as-fabricated double-clamped BLG device.
- fig. S2. Measurement showing BLG pulled into the bottom electrode.
- fig. S3. Relative changes in the resistance response of BLG plotted in Fig. 2B.
- fig. S4. Additional measurements of the resistance time revolution of current annealing regenerated the suspended BLG.
- fig. S5. Gate modulation of an additional suspended BLG in a CO₂ environment.
- fig. S6. Simulated charge density difference distribution in freestanding BLG, with one CO₂ adsorption event occurring in a large supercell.
- fig. S7. Model used in semiempirical molecular dynamics simulations.
- DFT calculations with vdW correction.
- References (32, 33)

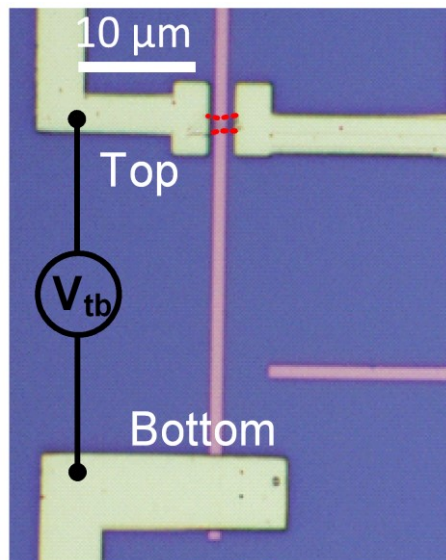


fig. S1. Optical microscopic image of the as-fabricated double-clamped BLG device. Red dot-lines highlight the edges of the BLG ribbon.

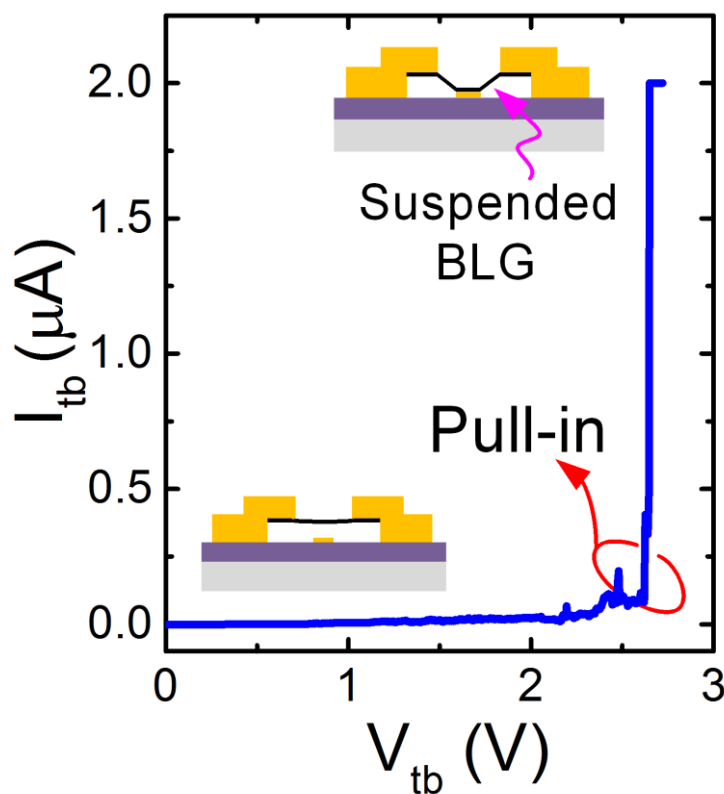


fig. S2. Measurement showing BLG pulled into bottom electrode. Insets are the schematics of the cross-sections of the device before and after the pull-in of graphene. A varied voltage V_{tb} increasing from 0 V was applied between top and bottom electrodes, as shown in fig. S1. At low V_{tb} , only leakage current of pico-ampere was measured, implying the suspension of graphene over the bottom electrode (see the lower inset), namely an open circuit. At 2.7 V, the current abruptly increased, which indicates the physical deflection of graphene onto the bottom electrode; this phenomenon is known as the pull-in effect.

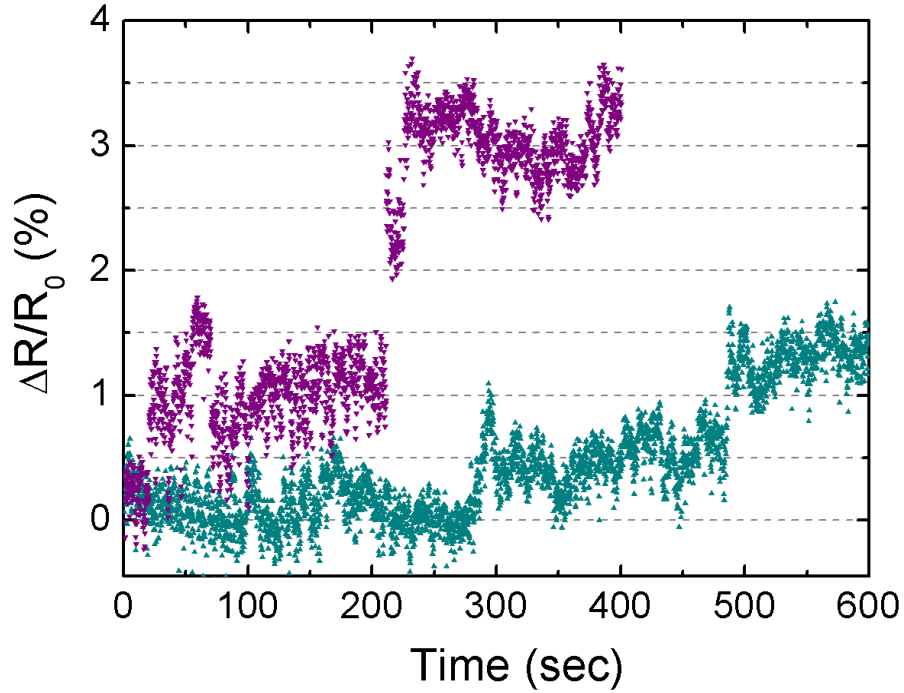


fig. S3. Relative changes in the resistance response of BLG plotted in Fig. 2B. Relative resistance change is defined as $\Delta R/R_0$ with R_0 being the initial resistance at the beginning of measurement. The absolute change ΔR of $\sim \pm 61 \Omega$ corresponds to a $\sim \pm 0.6\%$ relative change.

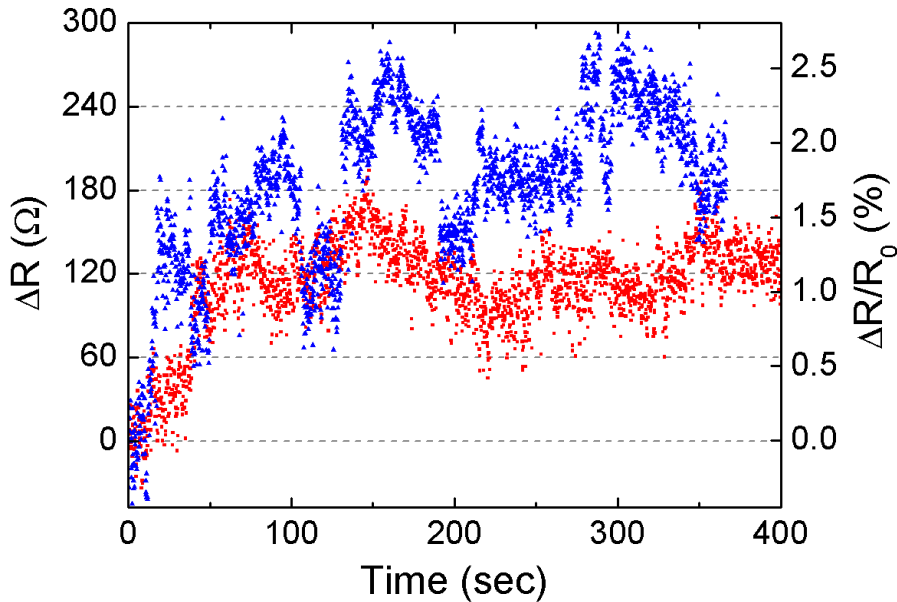


fig. S4. Additional measurements of the resistance time revolution of current annealing regenerated the suspended BLG. Back-gate voltage V_g was set at 15 V. These measurements were performed with the short current annealing regenerated device after the one of $V_g = 15 \text{ V}$ showed in Fig. 2B. The step-like resistance changes are again observed.

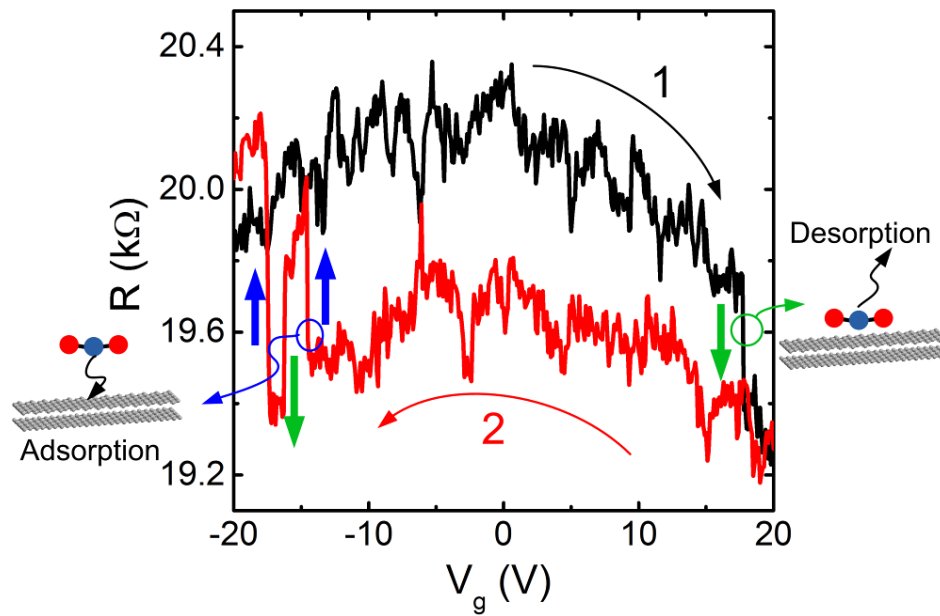


fig. S5. Gate modulation of an additional suspended BLG in a CO₂ environment. The abrupt step-changes occur during gate voltage sweeping, which can be ascribed to a few simultaneous physisorption/desorption events (positive and negative change correspond to adsorption and desorption, respectively.). After adsorption/desorption, the gate modulation curve with identical shape and CNP value compared with the one before adsorption is still measured with a clear resistance increment. This measurement serves as additional verification of the proposed scenario giving rise to the measured signal of adsorption (see Fig. 4B).

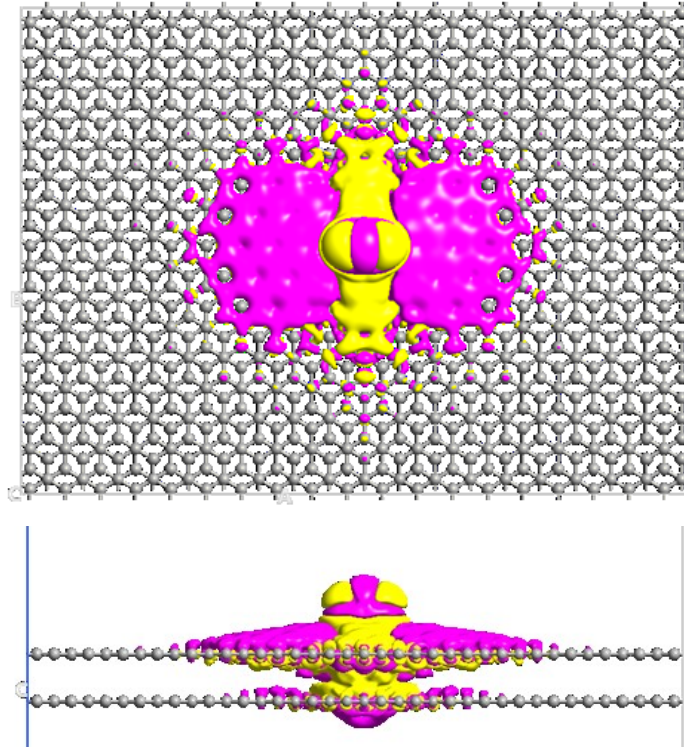


fig. S6. Simulated charge density difference distribution in freestanding BLG, with one CO₂ adsorption occurring in a large supercell (46.73 Å × 34.10 Å × 25 Å). Yellow and pink denote electron density enrichment and depletion with isovalue of $1 \times 10^{-6} \text{ e}/\text{Å}^3$, respectively. The charged impurity due to one CO₂ molecule spreads to $\sim 3 \text{ nm}$ wide area. Even though this structure was simulated for larger BLG supercell and using different DFT simulator, charged impurity affected area is consistent with plane wave DFT simulated results given in main text. We can clearly see the impact of charged impurity spreading to bottom layer of BLG as well from the side-view plot, which clearly indicates the blocking of carrier transport at the CO₂ adsorption site.

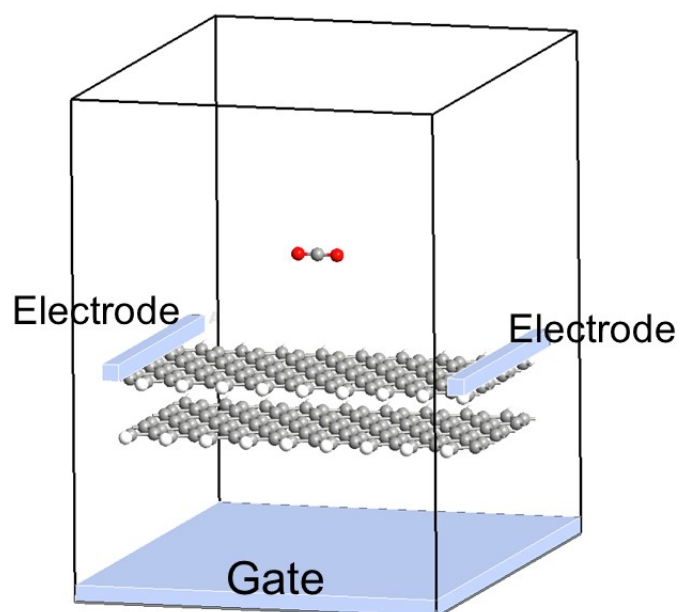


fig. S7. Model used in semiempirical molecular dynamics simulations. Simulated supercell structure for semiempirical molecular dynamics (254 atoms). Substrate potential was applied through gate electrode. In the CO₂ molecule adsorbed location, BLG will be flat locally. So, we have considered flat BLG in the molecular dynamics.

DFT calculations with vdW Correction

(a) CO₂–BLG/SiO₂ structure

SiO₂ substrate was simulated with simple cubic structure of SiO₂ with 1.5% strain. For the defective SiO₂ substrate, three oxygen vacancies were artificially introduced. SiO₂ slab was fixed in position during calculations. Supercell size of 17.05 Å × 19.69 Å × 30 Å was used in order to make sure a more than 10 Å vacuum space between adjacent cell in the vertical direction. As the supercell with 643 atoms is computationally heavy, we therefore applied Generalized Gradient Approximation (GGA) with Perdew Burke Ernzerhof (PBE) exchange and correlation functionals in SIESTA with single zeta polarized basis sets.

(b) CO₂–free-standing BLG structure

In order to accurately calculate the distributed area of charged impurity effect due to the adsorbed CO₂ molecules, super cell size of 27.07 Å × 34.10 Å × 25 Å was used in CO₂–BLG simulation, which contains 707 atoms in total. These dimensions make sure that the distance between adjacent bilayer graphene layers is greater than 10 Å. The k-point was set to 5 × 5 × 1 for the Brillouin zone integration.

(c) Larger size CO₂–BLG structure:

For further verification of the impurity expansion of adsorbed CO₂ molecule, simulation with a larger super cell size of 46.73 Å × 34.10 Å × 25 Å was also conducted, which contains 1219 atoms in total. This first-principle calculation was performed using Atomistrix ToolKit (version 2015.0, QuantumWise) [28,31], which is based on a linear combination of numerical atomic orbitals and normconserving Troullier–Martins pseudo-potentials. The Perdew–Burke–Ernzerhof exchange correlation functional, derived within the generalized gradient approximation, was applied. To take care of van der Waals interactions more accurately, Grimme dispersion correction was used when calculating dispersion forces [32]. Double zeta plus polarized basis sets were used in all of these calculations. The simulation results are plotted in fig. S6.